The Plant Cell, Vol. 18, 3106–3120, November 2006, www.plantcell.org © 2006 American Society of Plant Biologists

Lack of the Light-Harvesting Complex CP24 Affects the Structure and Function of the Grana Membranes of Higher Plant Chloroplasts [OA]

László Kovács,[a,1] Jakob Damkjær,[b] Sami Kereïche,[c] Cristian Ilioaia,[a] Alexander V. Ruban,[a,2] Egbert J. Boekema,[c] Stefan Jansson,[b] and Peter Horton[a,3]

[a] Department of Molecular Biology and Biotechnology, University of Sheffield, Sheffield S10 2TN, United Kingdom
[b] Umeå Plant Science Centre, Department of Plant Physiology, Umeå University, S-901 87 Umeå, Sweden
[c] Department of Biophysical Chemistry, Groningen Biomolecular Sciences and Biotechnology Institute, University of Groningen, 9747 AG Groningen, The Netherlands

The photosystem II (PSII) light-harvesting antenna in higher plants contains a number of highly conserved gene products whose function is unknown. *Arabidopsis thaliana* plants depleted of one of these, the CP24 light-harvesting complex, have been analyzed. CP24-deficient plants showed a decrease in light-limited photosynthetic rate and growth, but the pigment and protein content of the thylakoid membranes were otherwise almost unchanged. However, there was a major change in the macroorganization of PSII within these membranes; electron microscopy and image analysis revealed the complete absence of the $C_2S_2M_2$ light-harvesting complex II (LHCII)/PSII supercomplex predominant in wild-type plants. Instead, only C_2S_2 supercomplexes, which are deficient in the LHCIIb M-trimers, were found. Spectroscopic analysis confirmed the disruption of the wild-type macroorganization of PSII. It was found that the functions of the PSII antenna were disturbed: connectivity between PSII centers was reduced, and maximum photochemical yield was lowered; rapidly reversible nonphotochemical quenching was inhibited; and the state transitions were altered kinetically. CP24 is therefore an important factor in determining the structure and function of the PSII light-harvesting antenna, providing the linker for association of the M-trimer into the PSII complex, allowing a specific macroorganization that is necessary both for maximum quantum efficiency and for photoprotective dissipation of excess excitation energy.

INTRODUCTION

Photosynthesis is dependent on the collection of sunlight by groups of protein-bound chlorophylls and carotenoids, which make up the light-harvesting antenna. For photosystem II (PSII) in higher plants, this antenna is composed of the core pigment protein complexes CP47, CP43, and light-harvesting complex II (LHCII) (Green and Durnford, 1996). The latter are referred to as the peripheral antenna since they are located further away from the reaction center. The peripheral antenna is composed of a number of different proteins encoded by the *Lhcb* genes (Jansson, 1994). The major proteins are Lhcb1-6, which associate with pigments to form the complexes CP24, CP26, CP29, and LHCIIb. CP24, CP26, and CP29 are monomeric, but LHCIIb is a trimeric complex composed of mixtures of the Lhcb1-3 proteins and binds ~60% of the PSII chlorophyll (Peter and Thornber, 1991). Each PSII reaction center is associated with between two and four trimers depending on plant material and light conditions. The LHCII antenna is associated with a dimeric reaction center core (C_2) to give rise to a highly conserved structural unit, the C_2S_2 LHCII-PSII supercomplex, consisting of two copies each of CP26, CP29, and two LHCIIb trimers of the S type (reviewed in Dekker and Boekema, 2005). Further antenna complexes associate with this supercomplex to give rise to $C_2S_2M_2$ supercomplexes, which contain in addition two copies of CP24 and a further two LHCIIb trimers of the M type (see Figure 3A for a diagrammatic representation). In the grana membranes, supercomplexes are associated together into various megacomplexes, sometimes in higher-order semicrystalline arrays (Boekema et al., 2000). Such macrodomains are thought to provide extensive and efficient long-range energy transfer between photosystems that includes interaction even between domains on opposing pairs of membranes in the granum (Dekker and Boekema, 2005). This macroorganization of PSII seems to be functionally important; for example, when the main LHCIIb trimers are removed by genetic manipulation, the normally minor monomeric CP26 complex accumulates in larger amounts and is assembled in trimeric form into the megacomplexes (Ruban et al., 2003).

[1] Current address: Institute of Plant Biology, Biological Research Center, Hungarian Academy of Sciences, H-6726 Szeged, Temesvári krt. 62, Hungary.
[2] Current address: School of Biological and Chemical Sciences, Queen Mary University of London, London E1 4NS, UK.
[3] To whom correspondence should be addressed. E-mail p.horton@sheffield.ac.uk; fax 44-114-222-2712.
The author responsible for distribution of materials integral to the findings presented in this article in accordance with the policy described in the Instructions for Authors (www.plantcell.org) is: Peter Horton (p.horton@sheffield.ac.uk).
[OA] Open Access articles can be viewed online without a subscription.
www.plantcell.org/cgi/doi/10.1105/tpc.106.045641

Considerable attention has been given to the question of why there are so many different but very similar proteins in the LHCII antenna. In general terms, it has been hypothesized that this diversity arises from the requirement of dynamic aspects of PSII function; because of fluctuations in the spectral quality and intensity of sunlight and temporal variations in other environmental and metabolic factors, the PSII antenna needs to be able to harvest light efficiently when it is limiting but dispose of the excess energy when it is saturating (Horton et al., 1996; Bassi and Caffarri, 2000; Horton and Ruban, 2005). Thus, plants are able to not only adjust the composition of the antenna but also to reversibly switch between a light-harvesting and a dissipative state. The adjustment in composition involves changes in gene expression and protein turnover (Anderson et al., 1995; Montane et al., 1998), whereas covalent modification of LHCII proteins by phosphorylation modulates their interaction with PSII and photosystem I (PSI), a process known as the state transitions (Allen and Forsberg, 2001; Haldrup et al., 2001). Energy dissipation is observed as the nonphotochemical quenching (NPQ) of chlorophyll fluorescence. NPQ is a heterogeneous process. but the main component, the qE-type of NPQ, is induced in excess light because of the increase in the thylakoid ΔpH (Briantais et al., 1979). The acidification of the thylakoid lumen activates the enzymatic deepoxidation of LHCII-bound violaxanthin into zeaxanthin (Demmig-Adams, 1990) and is also thought to result in protonation of key amino acid residues within the LHCII antenna (Walters et al., 1996; Li et al., 2004). Together, these two events activate a process of energy dissipation. The PSII-associated protein, PsbS, a four-helix member of the Lhc gene family, plays a vital role in this process (Li et al., 2000).

Therefore, it has been proposed that the different compliment of Lhcb proteins is needed to enable these regulations of light-harvesting function to take place. For example, in plants, only Lhcb1 and Lhcb2 are phosphorylated after the state transition (Allen, 1992), and in the absence of these proteins, the transition is inhibited (Andersson et al., 2003). In the case of NPQ, existing data give a less clear conclusion. Elimination of Lhcb1 and Lhcb2 led to ~30% reduction in NPQ capacity (Andersson et al., 2003), but interpretation of this result is complicated by the compensatory change in CP26. In the absence of CP26, there was negligible change in NPQ, whereas in the absence of CP29, there was some small loss of NPQ, but only in low light (Andersson et al., 2001). In this article, we describe the investigation of plants in which the level of CP24 has been reduced either with a knockout mutation in the *Lhcb6* gene or in which *Lhcb6* gene expression has been reduced by expression of the corresponding antisense gene. The function of this complex had hitherto been unknown, but the ease of its removal from PSII core (Camm and Green, 1989) and its location in the more external part of the megacomplex (Dekker and Boekema, 2005) would support a hypothesis that its function was entirely regulatory. Moreover, the absence of this protein had a particularly strong effect on fitness, observed when plants depleted in this complex were grown in the field (Ganeteg et al., 2004). Here, we show that not only does the absence of this protein profoundly alter the macroorganization of the PSII antenna, but its absence affects both of the regulatory functions of the LHCII antenna, NPQ, and state transitions.

RESULTS

A Series of Plants with Lhcb6 Levels Ranging from 0 to 100%

The Lhcb protein composition of the *asLhcb6* line has been determined by Ganeteg et al. (2004), but it was necessary to ensure that the T-DNA knockout line for the *Lhcb6* gene (*koLhcb6*) had the same phenotype. Immunoblotting of thylakoids isolated from the *Lhcb6* knockout line (*koLhcb6*) showed, as expected, that there was no detectable Lhcb6 protein, and on a chlorophyll basis, there were no marked changes in the levels of any other Lhcb protein in *koLhcb6* compared with the wild type (Figure 1A). Only for Lhcb3 was there any difference, there being a 30% decrease in the mutant compared with the wild type. There was no change in the level of the PsbS protein or of the PsbA (D1) PSII reaction center protein. Apparently, the effect of removing CP24 by means of antisense inhibition or T-DNA insertion produced plants with the same phenotype. However, a large amount of variation in the various phenotypic characteristics of plants of the *asLhcb6* line was noted (see below). Therefore, a population of *asLhcb6* plants was analyzed for the level of Lhcb6. The extent of reduction showed considerable variation between plants: some plants had almost no CP24 protein, whereas others had levels approaching the wild type (Figures 1B and 1C). Taken together, we therefore had the possibility to analyze a whole series of plants, with Lhcb6 levels ranging from 100% (wild type) to 0% (*koLhcb6*). All phenotypic effects recorded during the further photosynthetic characteristics of the plants were stronger in plants having less CP24, and in the following, only data from antisense plants with strongly reduced levels of CP24 will be reported. However, in some analyses, advantage was made of plants having different amounts of CP24 depletion, and these will be mentioned specifically in the text.

Lhcb6 Depletion Caused a Reduction in Growth and Light-Limited Photosynthetic Rate

The chlorophyll content per leaf area was not changed by the depletion of CP24 (Table 1). Mature plants could not be distinguished visibly, and the photosynthetic rate at saturating light was the same. However, the photosynthetic rate in limiting light was slightly depressed in the plants lacking CP24, and there was a reduction in growth rate of the *koLhcb6* plants compared with the wild type: the rate of increase in rosette diameter was slower, the average time for flowering increased by several days, and the fresh weight was lower (Table 1).

Lhbc6 Depletion Did Not Cause a Major Change in Chloroplast Ultrastructure or the Composition of Pigments and Pigment Protein Complexes

Electron microscopy of thin sections revealed no significant differences in the appearance of the chloroplasts. Grana membranes were present in plants possessing reduced levels of CP24, and no significant differences in the size or frequency of appressed membranes was observed (data not shown). Pigment analysis indicated that the contents of chlorophylls

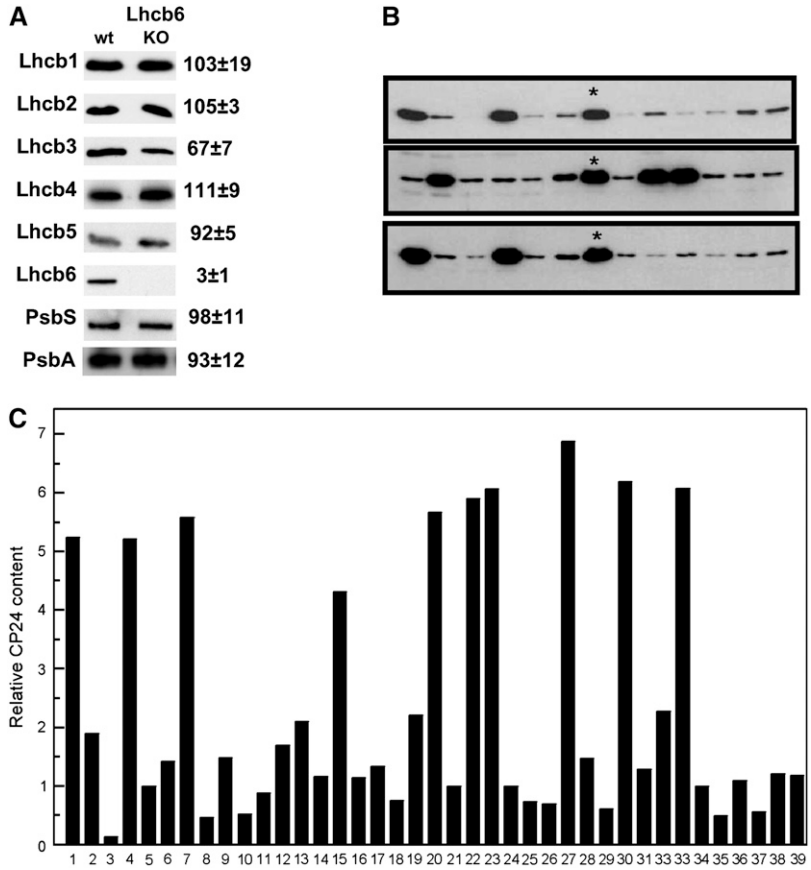

Figure 1. Content of Lhcb6 in Antisense and T-DNA Insertion Mutant Plants.

(A) Protein gel blots of wild-type and *koLhcb6* plants against antibodies to a range of PSII proteins. The amount of each protein, expressed as percentage of wild type, was determined from densitometry of between three and five replicate blots. Gels were loaded with equal chlorophyll. KO, knockout.

(B) Protein gel blots of different plants in the population of the *asLhcb6* line against Lhcb6 antibody. Asterisks indicates a wild-type plant included in each gel.

(C) Content of Lhcb6 from protein gel blots in the range of antisense plants, expressed as densitometric intensity on an equal chlorophyll basis. Data were obtained from the three gels shown in **(B)**.

and carotenoids were essentially identical in the plants deficient in Lhcb6 and the wild type (Table 1). There was no change in the chlorophyll *a*/*b* ratio and no change in the content of various xanthophylls. There was no difference in the extent light-induced deepoxidation of the xanthophyll cycle pigments. Since CP24 binds only a small fraction of thylakoid chlorophyll, no measurable change is expected from the absence of this complex. Rather, the data confirm that there are no major changes in the levels of other pigment protein complexes (e.g., in the PSI/PSII ratio or in the ratio of antenna over core complexes).

Gel filtration of detergent solubilized thylakoids confirmed the presence of the major pigment protein complexes in the CP24-depleted plants. Figure 2 shows the gel filtration chromatograms of solubilized thylakoid membranes obtained from wild-type and *koLhcb6* plants, recorded at 670 nm to monitor chlorophyll content. The elution profile of the wild-type plant (solid line) shows a strong similarity to that obtained previously (Ruban et al., 2006), and the compositions of these fractions were confirmed by observation of their absorption spectra (data not shown). The first two fractions (I and II) are attributed to grana membrane fragments and PSII-LHCII supercomplexes, respectively. Fraction III is assigned to monomeric PSI-200 complexes, and Fraction IV arises from PSII core monomers. Fractions V and VI originate from the major, trimeric LHCII and from monomeric LHC complexes, respectively. The chromatogram from the *koLhcb6* plants was broadly similar to the wild type, although some differences were consistently observed in the relative contributions of some bands (Figure 2, dashed line). There was always an increase in the amount of chlorophyll in the LHCII trimer Fraction V in the knockout line, indicating that some LHCII trimers were bound less tightly to the PSII core. Thus, although the composition may be almost the same, the CP24-depleted plants may exhibit some changes in the macroorganization of LHCII/PSII.

Table 1. Growth Parameters, Photosynthetic Rate, and Pigment Composition of CP24-Depleted Plants

	Growth Rate (mm/d)	Flowering Time (d)	Fresh Weight (g)	Chlorophyll (μg/cm²)	Chlorophyll *a*/*b*	Photosynthetic Activity (μmol CO_2 m^{-2} s^{-1})	
						LL	HL
Wild type	4.61 ± 0.18 ($n = 13$)	35.6 ± 0.83 ($n = 14$)	6.86 ± 0.66 ($n = 4$)	35.8 ± 1.4 ($n = 6$)	3.26 ± 0.04 ($n = 6$)	10.3 ± 0.24 ($n = 6$)	16.50 ± 0.22 ($n = 5$)
koLhcb6	3.85** ±0.16 ($n = 13$)	41.4** ±0.65 ($n = 9$)	4.82** ±0.46 ($n = 4$)	33.1 ± 1.3 ($n = 6$)	3.31 ± 0.03 ($n = 6$)	8.70** ± 0.44 ($n = 6$)	15.94 ± 1.22 ($n = 5$)
asLhcb6	ND	ND	ND	32.0 ± 1.3 ($n = 6$)	3.28 ± 0.11 ($n = 6$)	8.25* ± 1.03 ($n = 5$)	15.62 ± 1.21 ($n = 4$)

				Vio		Ant		Zea		
	Neo	Lut	β-Car	D	L	D	L	D	L	XC
Wild type	4.68 ± 0.15	15.46 ± 0.98	10.89 ± 0.34	4.13 ± 0.97	1.28 ± 0.15	0.20 ± 0.05	0.43 ± 0.14	0.009 ± 0.003	2.23 ± 0.36	4.33 ± 0.94
koLhcb6	4.99 ± 0.25	15.31 ± 0.39	10.87 ± 0.06	4.32 ± 0.22	1.10 ± 0.04	0.25 ± 0.03	0.66 ± 0.05	0.007 ± 0.008	2.75 ± 0.34	4.58 ± 0.20
asLhcb6	4.77 ± 0.03	15.20 ± 0.83	10.60 ± 0.86	3.76 ± 1.17	1.01 ± 0.39	0.24 ± 0.08	0.47 ± 0.24	0.027 ± 0.024	2.23 ± 0.17	4.03 ± 1.07

Growth rate was the increase in rosette diameter during the linear phase of growth. Flowering time was estimated as when a bolt of 1 cm was produced. Photosynthetic activity was determined at 250 (low light [LL]) and 1500 (high light [HL]) μmol photons m^{-2} s^{-1}. Values in the top part of the table are ± SE, with significant differences indicated by two asterisks (95% confidence limit) or one asterisk (90% confidence limit). Carotenoid content is expressed as mols/100 mols chlorophyll *a*/*b* ± SD ($n = 3$). Neo, neoxanthin; lut, lutein; β-car, β-carotene; vio, violaxanthin; ant, antheraxanthin; zea, zeaxanthin. XC is the total xanthophyll cycle pool. D, dark adapted leaves; L, leaves illuminated with 1500 μmol photons m^{-2} s^{-1} for 30 min. There were no significant differences between the D and L values for the nonxanthophyll cycle carotenoids. ND, not determined.

The Absence of CP24 Changed the Macroorganization of the Photosynthetic Membrane

Investigation of the structure of the grana membranes was then performed. The strategy used for structural analysis involved very mild detergent treatment of thylakoid membranes, followed by rapid fractionation by gel filtration (van Roon et al., 2000), similar to that used for Figure 2 but with a lower concentration of *n*-dodecyl α-D-maltoside (α-DM) to preserve the grana membranes and PSII supercomplexes, as successfully used previously to analyze the effects of depletion of other PSII LHCs (Ruban et al., 2003; Yakushevska et al., 2003). The samples are then immediately prepared for electron microscopy analysis. Although this procedure does not yield highly purified samples, this is not critical for electron microscopy analysis because the applied image analysis procedures allow the projections of single PSII molecules and eventual contaminants to be classified. Moreover, the major advantage of this procedure is that membrane fragments containing ordered arrays of PSII complexes can also be obtained in the same gel filtration fraction. This allows an analysis of the supercomplex structure and the macroorganization of the complexes in the thylakoid membrane to be obtained simultaneously.

The supercomplex population was analyzed by single particle electron microscopy. Figure 3A shows a model of the $C_2S_2M_2$ supercomplex in which the structure of the PSII core dimer has been fitted and the M and S LHCIIb trimers are shown together with the three minor complexes, CP24, CP26, and CP29 (Dekker and Boekema, 2005). Surprisingly, classification of a set of 2000 single particle projections from the *koLhcb6* plants revealed that >95% consisted of the C_2S_2 supercomplex (Figure 3B). These supercomplexes were identical to those previously observed as a minor population in wild-type *Arabidopsis thaliana* (Figure 3D) and do not contain CP24. $C_2S_2M_2$ and C_2S_2M, the larger supercomplexes with either one or two M-type LHCII trimers, which are the predominant supercomplexes in spinach (*Spinacia oleracea*) (Boekema et al., 1999a) and wild-type *Arabidopsis*, respectively (Figures 3E and 3F; Yakushevska et al., 2001), were

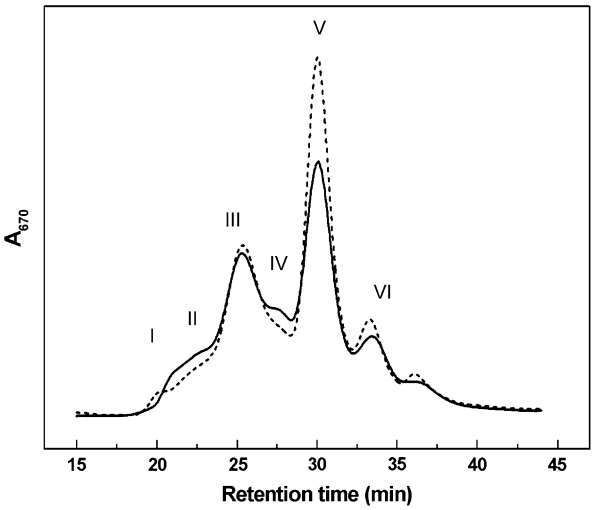

Figure 2. FPLC Gel Filtration Fractionation of Solubilized Wild-Type and Mutant *koLhcb6* Thylakoid Membranes.

Chromatograms of solubilized thylakoids from the wild type (solid line) and *koLhcb6* (dashed line). Major fractions are marked as follows: PSII membrane fragments (I), PSII supercomplexes (II), PSII core complexes (IV), PSI complex (III), and trimeric (V) and monomeric (VI) LHCs. Thylakoids were solubilized with 0.7% α-DM.

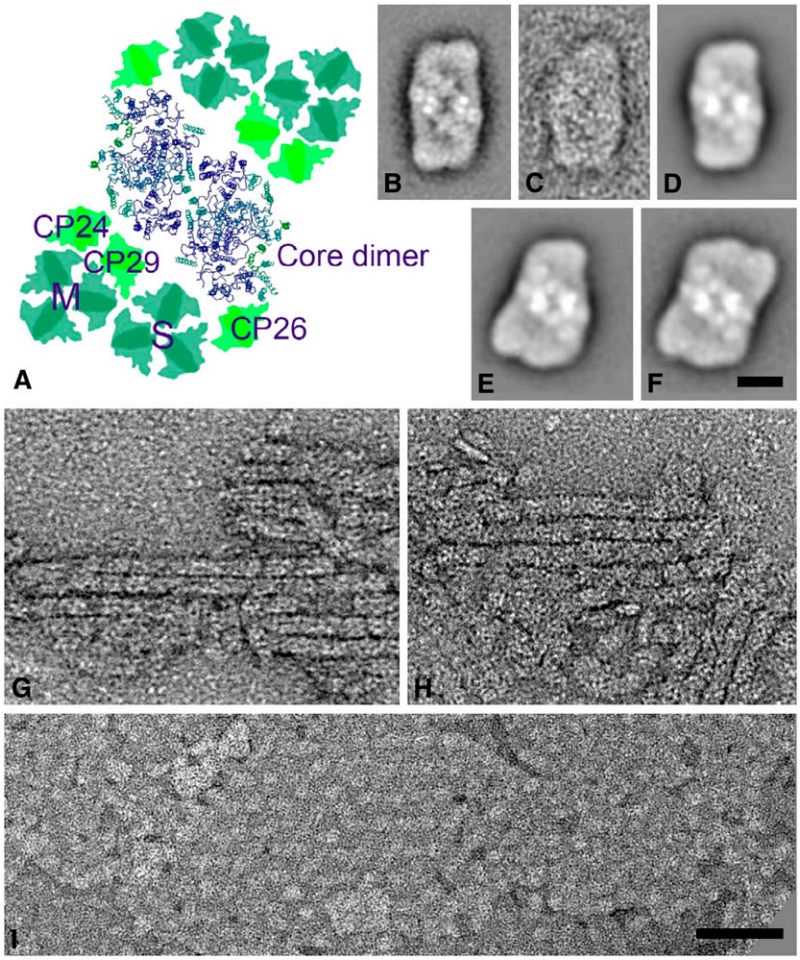

Figure 3. Electron Microscopy of PSII Particles and Grana Membranes.

(A) Model of the $C_2S_2M_2$ supercomplex showing the fitting of the high-resolution structural model of the PSII core dimer, the CP24, CP26, and CP29 minor complexes (pale green), and the M and S LHCIIb trimers (green) (from Dekker and Boekema, 2005).
(B) Average projection map of best 500 projections of a set of ~2000 C_2S_2 supercomplexes from the plants lacking CP24.
(C) Average projection map of 10 projections of C_2S_2 supercomplexes lacking one CP26 subunit at the top left tip from the plants lacking CP24.
(D) to **(F)** Projection maps of C_2S_2, C_2S_2M, and $C_2S_2M_2$ supercomplexes found in wild-type plants (reproduced from Yakushevska et al., 2001)
(G) and **(H)** Partially solubilized grana membranes from plants lacking CP24, showing ordered arrays of C_2S_2 supercomplexes.
(I) Partially solubilized grana membranes from wild-type plants, showing ordered arrays of $C_2S_2M_2$ supercomplexes.
Thylakoids were solubilized with 0.6% α-DM. Bars = 10 nm in **(B)** to **(F)** and 100 nm in **(G)** to **(I)**.

completely absent. A very small number (~1%) of C_2S_2 particles lacking one CP26 subunit were also present (Figure 3C) as well as some sandwiched supercomplexes in side-view position (data not shown). In *Arabidopsis*, almost all the C_2S_2 supercomplexes have both CP26 subunits attached, in contrast with spinach where a substantial number of complexes lack a CP26 subunit (Boekema et al., 1999b).

Grana membrane fragments were found to be partly composed of semicrystalline areas, which consisted of rows of supercomplexes in a head-to-tail arrangement along the rows (Figures 3G and 3H). This structure is completely different from the crystalline array found in the wild type (Figure 3I). This array has been analyzed previously (Yakushevska et al., 2001, 2003; Ruban et al., 2003) and was shown to consist of arrays of $C_2S_2M_2$ supercomplexes. The width of the rows in the image of the CP24-depleted membranes was 15.5 to 16 nm, which is identical to the width of the C_2S_2 supercomplex. Hence, they are considered to be composed of ordered arrays of C_2S_2 complexes. Areas of noncrystalline domains were also observed, such as in the left part of Figure 3H; these have a granularity similar to PSI domains found earlier (Boekema et al., 2000), which are quite different from the LHCII-only domain, which have a very smooth appearance (Boekema et al., 2000). Biochemical analysis indicated that there was no depletion of LHCII in the *koLhcb6* plants (see Figure 1). The crystalline domains were generally smaller in the samples depleted of CP24 compared with those of the wild type. Hence, they may be more disrupted than the wild type, and it is suggested that the nonbound LHCII trimers have been selectively

removed from these membranes by the detergent treatment. The presence of a more loosely associated population of LHCII would also explain the stronger LHCII trimer band in the gel filtration profile of the CP24-depleted plants (Figure 2).

Spectroscopy Analysis Confirmed the Alteration in PSII Macroorganization in the CP24-Depleted Plants

Circular dichroism (CD) spectroscopy is a sensitive noninvasive method to study the structural changes in the PSII supramolecular organization and was therefore used to further investigate the effects of CP24 depletion. Figure 4 shows the CD spectra of leaves (A) and isolated thylakoids (B) of the wild type and plants lacking Lhcb6. The CD spectra of leaves and isolated thylakoid suspensions were identical, showing that all the bands observed in thylakoid were present in intact leaves, and there was no distortion or artifact from the structural elements of leaf tissues.

The main CD bands of the wild-type leaf and thylakoid spectra in the red (at 690 nm) and blue (at 510 nm) region are the psi-type bands (Figures 4Aa and 4Bg). These large, anomalously shaped CD bands are not explained by short-range interactions of chromophores within individual pigment protein complexes but arise from the long-range interactions between them in large, chiral macromolecular domains (Keller and Bustamante, 1986). The presence of the psi-type CD bands in the CD spectra of wild-type leaves and thylakoid membranes indicates the expected existence of chiral LHCII-containing macrodomains of the pigment protein complexes in the granal membranes, estimated to be ~200 to 400 nm (Garab et al., 1988; Finzi et al., 1989). The minor bands in the spectrum at (−)653 nm, (+)485 nm, and (+)448 nm are excitonic bands arising from short-range interactions of the chromophores. Solubilization of the thylakoid membranes completely abolishes the psi-type CD bands (Figure 4Bh) by disruption of long-range interactions, revealing the conservatively shaped split signals attributed only to the short-range excitonic interactions of chlorophyll molecules (Dobrikova et al., 2003).

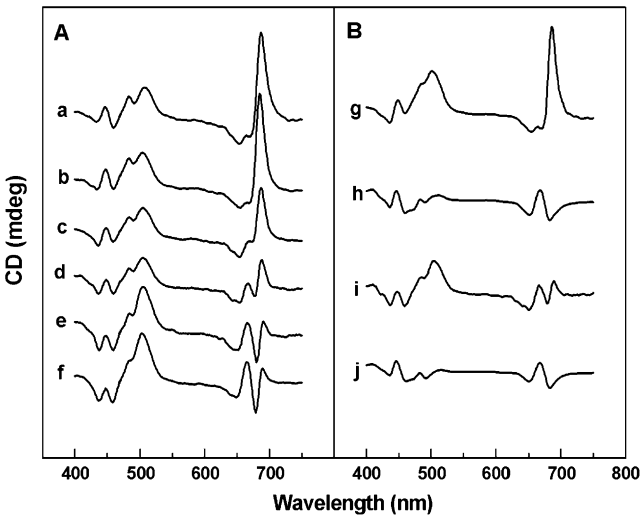

Figure 4. CD spectroscopy of Leaves and Thylakoid Preparations from the Wild Type and Plants Lacking CP24.

(A) Wild-type leaves **(a)**, *asLhcb6* leaves with different CP24 contents (**[b]** to **[e]**), and *koLhcb6 leaves* **(f)**.

(B) Wild-type thylakoids **(g)**, wild-type thylakoids solubilized with 0.01% β-DM **(h)**, *asLhcb6* thylakoids **(i)**, and *asLhcb6* thylakoids solubilized with 0.01% β-DM **(j)**.

Depletion of CP24 has a marked effect on the CD spectrum of the leaves and thylakoid membranes (Figures 4Af and 4Bi). The (+)690-nm psi-type band is completely missing from the spectrum of *koLhcb6* plants. This region of the spectrum exhibits only the split signals similar to that found in the solubilized wild-type thylakoid membrane. The 690-nm band was also significantly reduced in the *asLhcb6* leaves, but the extent of decrease showed a high deviation in different plants, similar to the deviation found in CP24 content (Figures 4Ab and 4Ae). Some *asLhcb6* plants exhibited a (+)690-nm band with an amplitude characteristic of the wild type (Figure 4Ab), while others were similar to the *koLhcb6* plants (Figure 4Ae). Neither the minor excitonic bands nor the (+)505-nm psi-type band in the Soret region changed significantly in either type of CP24-depleted plant modified lines compared with the wild type. Solubilization of the CP24-depleted thylakoid membranes with detergent results in CD spectra identical with the solubilized thylakoid membrane isolated from wild-type plants (Figure 4Bj), proving that the differences in the CD spectra measured in situ reflect the altered macroorganization of the pigment protein complexes of the thylakoid membrane.

The variable content of CP24 protein in *asLhcb6* plants provided the possibility to establish the correlation between the CP24 content of leaves and the macroorganization of thylakoid membrane monitored by CD spectroscopy. The amplitude of the (+)690-nm psi-type band of normalized CD spectrum plotted against the relative amount of CP24 protein is shown in Figure 5A. At lower CP24 levels, the (+)690-nm psi-type band shows approximately linear correlation with CP24 content, but at higher concentrations (~60% of the wild type), it saturates at the amplitude found in wild-type plants. The amplitude of the 448-nm excitonic band was independent of CP24 content.

The functional expression of the long-range organization of the PSII antenna into the macrodomain is the establishment of connectivity between PSII reaction centers. Thus, reaction centers can share the same light-harvesting system, and energy transfer can take place between large numbers of LHCII in the macrodomain. Connectivity is manifested in the sigmoidal kinetics of the fluorescence rise that accompanies light-induced primary electron accepting plastoquinone of PSII (Q_A) reduction and can be simply explained by the notion that excitation arriving at a closed center can transfer to an open one rather than being emitted as fluorescence (Lavergne and Trissl, 1995). The connectivity parameter J was found to be ~1.5 in wild-type plants (Table 2), in agreement with previous results (Nedbal et al., 1999). In the *koLhcb6* plants, the J parameter decreases to ~0.9. In the antisense plants, again there was a range of J values, between those found for the wild-type and *koLhcb6* plants (data not shown). The maximum quantum efficiency, Fv/Fm, was also lower in the plants depleted of CP24. This arose in part from the higher minimum level of fuorescence (Fo) in the CP24 mutants.

Low-temperature fluorescence spectroscopy of thylakoid membranes from wild-type and *koLhcb6* plants provided further

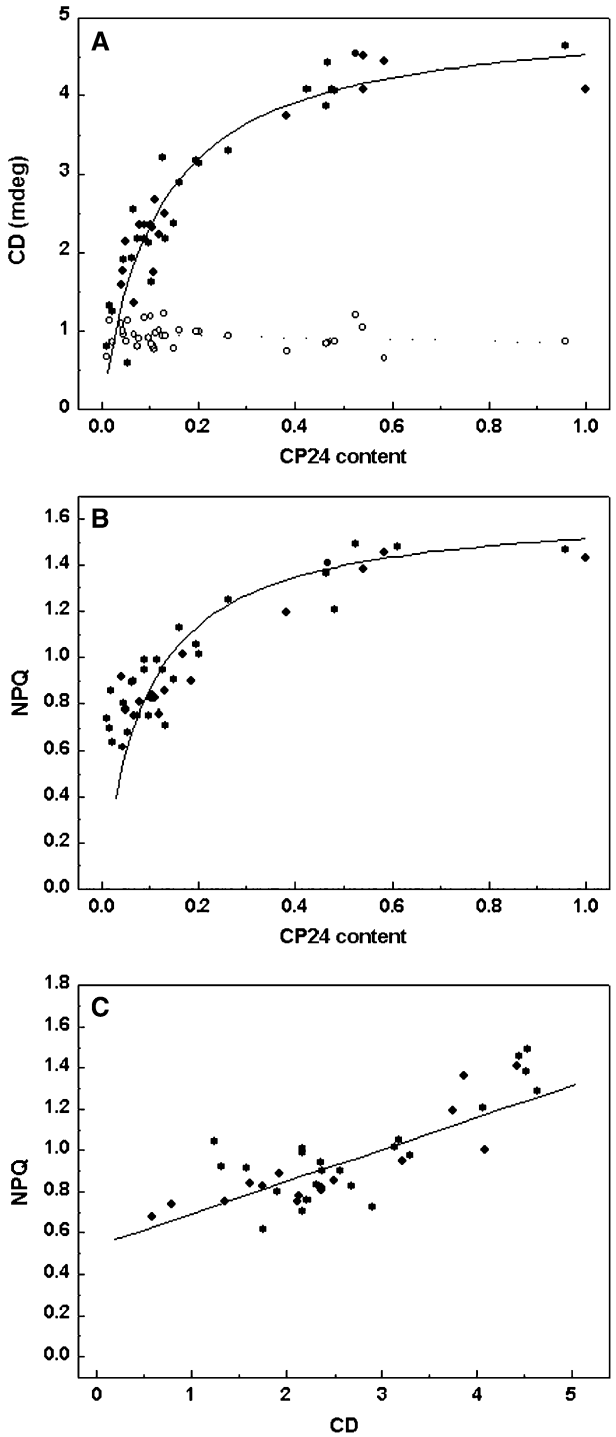

Figure 5. Relationship between Lhcb6 Protein Content and Spectroscopic Parameters of Thylakoid Structure and Function in *asLhcb6* Plants.

(A) Amplitude of CD bands at 690 nm (closed circles) and 448 nm (open circles) obtained from the spectra recorded in Figure 4, normalized to the amplitude of the (−)653-nm band and the relative CP24 content, assessed from densitometry of protein gel blots as shown in Figure 1 and normalized to the maximum amount (= 1).

(B) Value of reversible NPQ (qE) obtained as in Figure 7 and the CP24 content.

(C) Correlation between NPQ obtained as in Figure 7 and amplitude of CD obtained as in Figure 4.

evidence for a difference in the organization of the PSII antenna (Figure 6). The emission spectrum for wild-type thylakoids showed the three major bands at 685 and 695 nm (from the PSII core) and 735 nm from PSI (Figure 6A). A weak shoulder at ~680 nm corresponds to fluorescence directly from LHCIIb. In the CP24-depleted thylakoids, the spectrum was altered: the 680-nm emission was enhanced, while that from the PSII core bands was reduced. The excitation spectra for the 695-nm PSII emission were analyzed to identify the origin of the change (Figure 6B). The difference spectrum, wild type-minus-*koLhcb6*, contained several bands, all of which are diagnostic of LHCIIb trimers (Ruban et al., 2000): 438 nm (chlorophyll a), 472 nm (chlorophyll b), 485 (neoxanthin), 495 (lutein 1), and 510 nm (lutein 2). Thus, the changes in the emission spectrum in Figure 6A can be explained by a decrease in efficiency of energy transfer from LHCII to PSII and an associated increase in emission directly from LHCII itself.

Depletion of CP24 Resulted in a Reduction in NPQ

Fluorescence induction curves recorded on leaves are shown in Figure 7. As expected from previous results, the wild-type leaves (Figure 7A) showed rapidly forming NPQ, the majority of which reversed rapidly at the end of the illumination, indicating that it was the ΔpH-dependent qE type of NPQ. Illumination of leaves from plants lacking CP24 revealed a decreased tendency for NPQ formation (Figures 7B and 7C). Calculation of NPQ values showed that steady state levels were reached in all cases, and the difference between wild-type and CP24-deficient plants was in the extent of qE (Figure 7D). It was noted that the kinetics of NPQ formation were altered in the *koLhcb6* plants compared with the wild type; in the latter, the rapid rise in NPQ was followed by a slower phase, whereas in the mutant, the slower phase was almost completely absent. The full light intensity profile for the induction of qE is shown in Figure 8. The reduction in qE in the CP24-depleted plants was observed at all light intensities, with a maximum reduction of ~60% in the *koLhcb6* plants. Differences in NPQ were observed across a number of antisense plants, and these could be correlated again with the content of CP24 protein; plants with 50% of Lhcb6 were found to have wild-type levels of NPQ (Figure 5B). Analysis of the activity of the xanthophyll cycle revealed no difference between the wild type and the plants deficient in CP24; for the NPQ data shown in Figure 7, the deepoxidation state was 43.7 ± 1.9 in the wild type and 47.9 ± 5.1 in the CP24-depleted plants.

State Transitions Were Affected in the Absence of CP24

State transitions describe the ability of plants to adjust the relative rates of excitation of PSII and PSI by reversible dissociation of LHCII from PSII and its association with PSI (Haldrup et al., 2001). It is dependent upon the reversible phosphorylation of LHCIIb. The effect of state transitions on chlorophyll fluorescence in wild-type

Table 2. Fluorescence Induction Parameters Determined for Leaves of Wild-Type and CP24-Depleted Pplants

	Fo	Fm	Fv/Fm	J
Wild type	527.4 ± 20.4	2816.2 ± 132.2	0.81 ± 0.002	1.48 ± 0.11
asLhcb6	614.9 ± 12. 7	2530.8 ± 125.5	0.75 ± 0.005	ND
koLhcb6	683.3 ± 33.6	2534.3 ± 41.7	0.73 ± 0.012	0.93 ± 0.01

Fo, Fm, and Fv/Fm were recorded as described in Figure 7 but are the unnormalized values. Values are ± SD ($n = 6$). The connectivity parameter J was determined from fast fluorescence induction curves as described in Methods. ND, not determined.

plants is shown in Figure 9A. Illumination with red light, absorbed preferentially by PSII, results in the leaves reaching State II. This is characterized by a low Fm (Fm^{II}) because LHCII has been removed from PSII and a very small decrease in fluorescence when light absorbed by PSI (far red [FR]) is first applied (because the red light is almost equally exciting PSII and PSI, and no further oxidation of Q_A would be induced). When the illumination with FR is continued, the fluorescence slowly rises until State I is reached; here, the Fm (Fm^{I}) is now higher (because LHCII has reassociated with PSII), and turning off the FR light gives an immediate increase in fluorescence (because red light now excites PSII more than PSI, causing Q_A reduction). This is followed by a fluorescence decrease as the transition to State II is induced. In plants lacking CP24, the state transition is observed, but there are important differences (Figure 9B). First, the extent of the state transition when expressed by the difference between Fm^{I} and Fm^{II} was reduced. However, it should be noted that in the plants lacking CP24, State II was completely reached: a very small fluorescence decrease was observed when FR light was given. Second, the state transition was much faster in the plants lacking CP24. Thus, when the FR light is turned off in State I, the induction of State II occurs rapidly and is complete within 3 min. By contrast, in the wild type, this takes at least 10 min. The transition from State II to State I was also faster in the *koLhcb6* plants.

DISCUSSION

CP24 Plays a Role in the Macrostructure of the Thylakoid Membrane

In the grana membranes of higher plant chloroplasts, PSII assumes a characteristic macroorganization. The minimum unit of LHCII/PSII, the C_2S_2 supercomplex, can be augmented with additional LHCs to form various larger supercomplexes, the most predominant of which in *Arabidopsis* are the C_2S_2M and $C_2S_2M_2$ complexes (Yakushevska et al., 2001). The $C_2S_2M_2$ complex contains two PSII core complexes, four LHCII trimers, and two copies each of the minor antenna, CP24, CP26, and CP29. In the grana membranes, these complexes can form megacomplexes, frequently assembling into areas containing crystalline arrays of characteristic size and spacing (Boekema et al., 2000; Dekker and Boekema, 2005). The depletion of CP24 resulted in a profound change in PSII macrostructure: C_2S_2 supercomplexes replaced $C_2S_2M_{1\text{-}2}$ complexes as the predominant form of LHCII/PSII, and the crystalline arrays consisted of rows of C_2S_2 complexes giving rise to a radically different appearance. Thus, in the absence of CP24, the M-LHCII trimer is not associated with the supercomplex. It should be emphasized that the protein gel blots indicated that the content of every other antenna protein was maintained at wild-type levels. Apart from the decrease in Lhcb3 (which is thought to be part of the M-trimer), there was neither a significant loss of LHCII nor a compensatory increase in the levels of other complexes. Instead, PSII was organized into a different structural form without CP24 or the M-LHCII trimer. Most likely some of the nonbound LHCII will accumulate in LHCII-only domains, found frequently in spinach (Boekema et al., 2000). However, the *Arabidopsis* grana

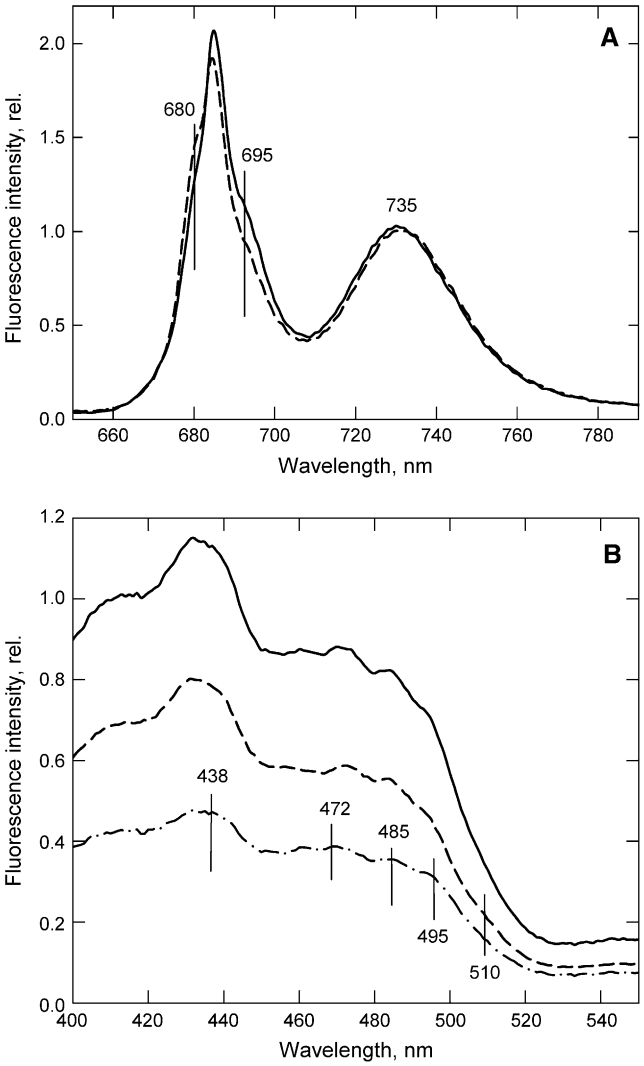

Figure 6. Low-Temperature Fluorescence Spectroscopy of Thylakoids from Wild-Type and CP24-Depleted Plants.

(A) Fluorescence emission spectra excited at 435 nm.
(B) Fluorescence excitation spectra for emission at 695 nm.
Solid line, wild type; dashed line, *koLhcb6*. Spectra were normalized to the intensity at 735 nm. In **(B)**, the difference spectrum, wild type-minus-*koLhcb6*, is displayed (dashed-dotted line).

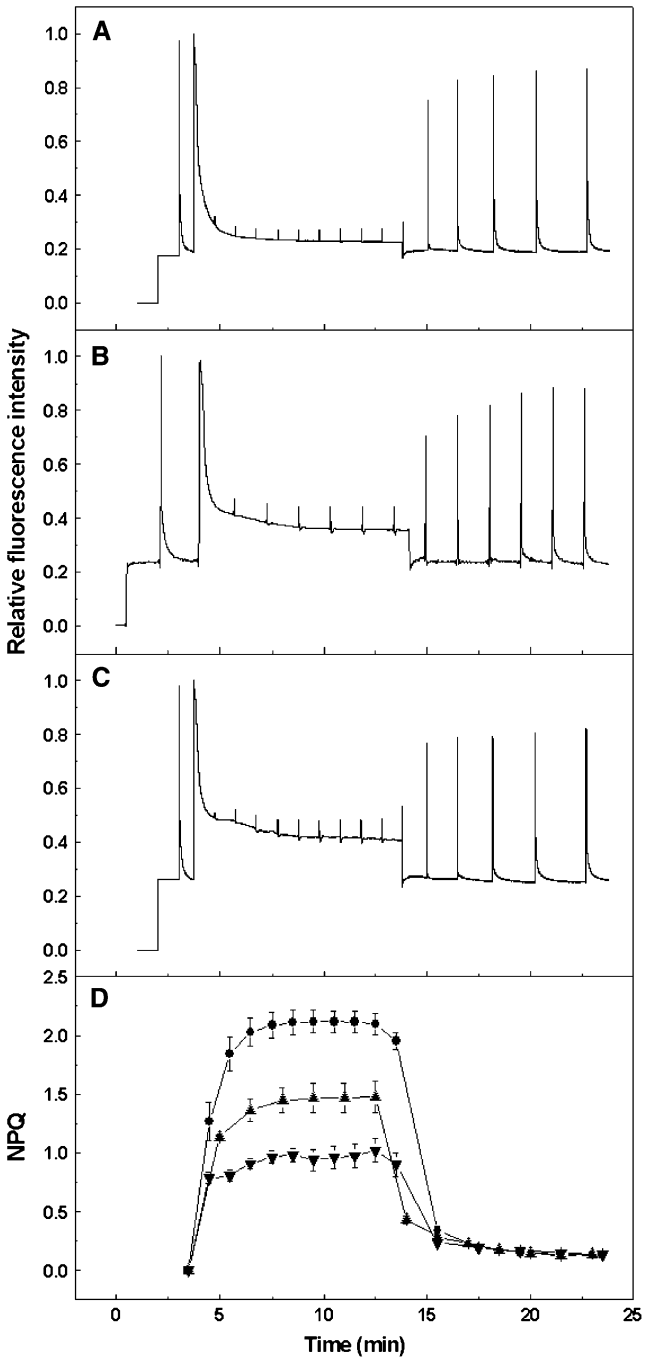

Figure 7. Effect of CP24 Depletion on Chlorophyll Fluorescence Quenching.

(A) Chlorophyll fluorescence traces recorded for wild-type leaves.
(B) Chlorophyll fluorescence traces recorded for *asLhcb6* leaves.
(C) Chlorophyll fluorescence traces recorded for *koLhcb6* leaves.
(D) NPQ induction and relaxation calculated from the data in **(A)** to **(C)**. Wild type, circles; *asLhcb6*, triangles; and *koLhcb6*, inverted triangles. Data are means ± SE of seven (wild type and *asLhcb6*) or eight (*koLhcb6*) replicates from different plants.
Actinic light, intensity 800 μmol photons m^{-2} s^{-1}, was given for 10 min followed by a 10-min dark period. In **(A)** to **(C)**, data are normalized to an Fm of 1.0.

membranes are overall less intact after detergent treatment than those of spinach, and likely most of the nonbound LHCII was selectively removed. Thus, the enhanced contribution of LHCII to the gel filtration chromatogram of the *koLhcb* plants arises because of the presence of a less tightly associated M-trimer population. Clearly, CP24 is an important component of the PSII antenna, whose presence influences the macroorganization of the granal membranes by providing the linker for association of the LHCII M-trimer into the PSII complex, allowing a different type of macroorganization.

CP24 Promotes Long-Range Chlorophyll Interactions in the Grana

In the grana membranes, there is long-range interaction between chlorophylls manifested by the appearance of the psi-type CD bands (Garab et al., 1988). This order can be reproduced in lamellar aggregates of LHCII (Simidjiev et al., 1997). This long-range order can be lost by removal of divalent cations (Barzda et al., 1994), detergent solubilization, and heat treatment (Dobrikova et al., 2003), in each case associated with the gross disturbance of the grana membranes, including destacking. Decrease in the amplitude of the psi-type CD bands also occurred following intense illumination, an effect attributed to a monomerization of LHCII trimers (Garab et al., 2002). In plants depleted of CP24, the psi-type CD was also lost, therefore indicating a decrease in long-range order, and by implication, a change in grana structure. This change would appear to be the shift from a $C_2S_2M_{1\text{-}2}$ macrostructure to a C_2S_2 macrostructure. It is important to note that depletion of CP24 only decreases the CD band in the red region of the spectrum, and the band at ~500 nm persists. This change therefore differs from those arising when destacking occurs, when all psi-type bands are lost. Hence, the main red band does not arise from stacking per se but depends upon the lateral

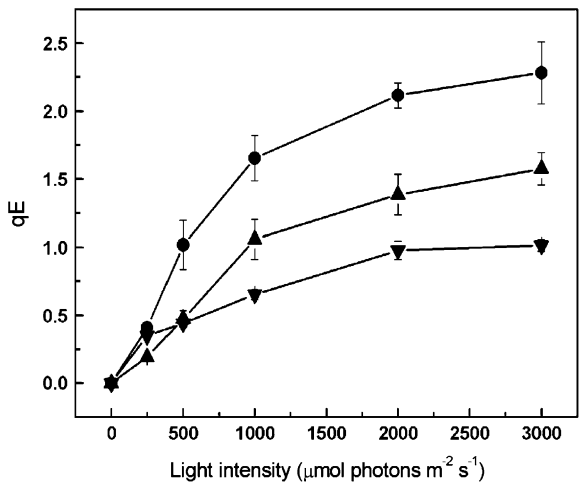

Figure 8. Rapidly Reversible qE Type of NPQ Recorded at Different Actinic Light Intensities.

Experiment performed as described in Figure 7. Wild type, circles; *asLhcb6*, triangles; and *koLhcb6*, inverted triangles. Data are means ± SE of between three and seven replicates using different plants.

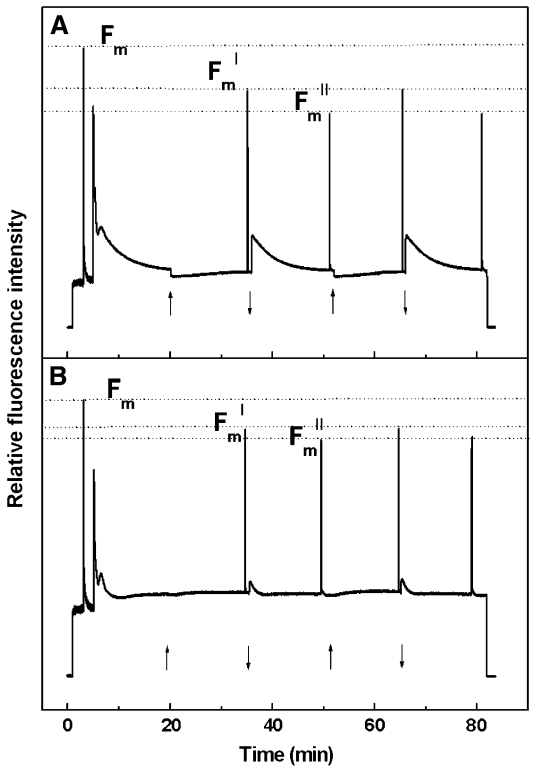

Figure 9. Effect of CP24 Depletion on State Transitions.

(A) Wild-type plants.
(B) *koLhcb6* plants.
Dark-adapted leaves were illuminated with PSII light to reach state II. Periods of PSI light were given (upward arrow, on; downward arrow, off). Light saturation pulses were given to record Fm, Fm^I, and Fm^{II}.

organization of LHCII within the stacks and is perhaps a fingerprint of a $C_2S_2M_{1\text{-}2}$-containing macrostructure.

CP24 Depletion Has Major Functional Consequences

The LHCII antenna plays three physiological roles: it is responsible for increasing the absorption cross section of PSII and providing efficient delivery of excitation energy to PSII; by the process of reversible phosphorylation, it controls the equilibrium distribution of excitation between PSII and PSI; and it has been suggested to be the site of dissipation of excess excitation in the process of NPQ (Horton and Ruban, 2005). Our data show that CP24 plays a key role in each of these functions.

Light Harvesting

The content of LHCII is not significantly reduced in the absence of CP24; hence, any change in the efficiency of PSII has to result from altered organization, not composition. Two changes in antenna function were observed. First, there was a decrease in Fv/Fm, the maximum quantum yield of PSII. This change arose in part from an increase in Fo. Although this could arise from an alteration in the trapping efficiency of PSII reaction centers, this seems unlikely. Instead, the preferred explanation is that it arises because of some poorly coupled LHCIIb; the displaced M-trimers may not be able to transfer energy efficiently to PSII reaction centers, giving rise to an elevated Fo. The detection of enhanced emission at 680 nm in the low-temperature spectrum of *koLhcb* thylakoids provides evidence for the presence of this population of LHCIIb. The second difference between the CP24-depleted plants and the wild type lay in the value of the connectivity parameter J. This parameter is the probability of excitation energy arriving at a closed PSII center being trapped by a neighboring open one. It describes the extent to which the PSII antenna can be described as a lake where a large number of centers share the same antenna as opposed to a puddle where each center only receives energy from its own antenna (Lavergne and Trissl, 1995). A connectivity parameter of 1.5 was found in the wild type, as routinely found for higher plants and algae (Lazar, 1999; Nedbal et al., 1999), but it decreased to <1.0 in the CP24-depleted plants. It has been assumed that the assembly of LHCII/PSII complexes in the grana facilitates their connectivity. Here, we show that that connectivity is dependent upon the precise nature of this organization; a macrodomain containing $C_2S_2M_{1\text{-}2}$ complexes is needed for maximum connectivity, whereas a C_2S_2 structure has much reduced connectivity. Thus, it is suggested that the presence of the bound M-trimer facilitates the transfer of energy between neighboring PSII complexes. Because it has been postulated that the connectivity between centers is an adaptation to photosynthesis in limiting light, CP24 could be viewed as an attribute of the evolution of an antenna that maximizes the efficiency of light collection. This is consistent with the decreases in the growth rate and light-limited photosynthetic rate in the CP24-depleted plants.

State Transitions

State transitions are a further adaptation of plants to photosynthesis in limiting light (Horton et al., 1996). Since CP24 is not a substrate for the thylakoid protein kinase, its absence would not be predicted to affect the state transition. However, two aspects of the transition were altered. First, the extent of the transition was reduced in the CP24 mutant, when measured as the relative change in Fm. Second, the rate of the transition was faster than in the wild type. In terms of the reduced extent of the state transition, it is necessary to examine the details of the fluorescence trace to distinguish whether this arises because of an inhibition of the formation of State II or the inability to fully assume an initial State I. State II is defined as that state when the rates of excitation of PSII and PSI are balanced so that no further oxidation of PSII occurs when extra PSI-absorbed light is given. By this definition, State II was achieved in both the mutant and the wild type. Indeed, in the mutant, State II was even more complete since the FR-induced oxidation was virtually absent. Thus, the difference between the mutant and wild type is in State I, not the transition between State I and State II, which in fact proceeds more completely and more rapidly in the CP24-depleted plants than in the wild-type plants. The presence of a population of LHCIIb poorly coupled to PSII could again provide an explanation of this. Furthermore, it is suggested that the presence of an M-trimer–depleted form of LHCII/PSII is indicative of State II.

Indeed, examination of thylakoid membranes in State II has shown an increase in the proportion of $C_2S_2M_1$ complexes at the expense of $C_2S_2M_2$ complexes (Kouril et al., 2005), providing evidence that it is indeed the M-trimers that relocate from PSII to be coupled to PSI. The difference in the kinetics of state transitions in the plants lacking CP24 arises because the M-trimers are no longer tightly associated with the PSII supercomplex and hence are more easily able to dissociate from the granal membranes (Figure 10).

NPQ

The site and mechanism of the main reversible component of NPQ is not proven (Holt et al., 2004; Horton et al., 2005). The transthylakoid ΔpH is the primary factor, whereas for maximum NPQ in vivo, there is a requirement for violaxanthin deepoxidation to zeaxanthin and the PSII antenna protein PsbS. It has been suggested that neither zeaxanthin nor PsbS is obligatory for quenching; rather, they could act as positive regulators (Crouchman et al., 2006). Alternatively, it has also been proposed that PsbS and/or zeaxanthin are the quenching agents (Li et al., 2000; Holt et al., 2004). Irrespective of which mechanism proves to be the correct one, NPQ requires an interaction between these molecules and a chlorophyll binding protein. It has been suggested that the LHCIIb trimers provide this site because the amplitude of NPQ is reduced when LHCIIb is partially removed by genetic manipulation (Andersson et al., 2003) and because it is now proven that each LHCIIb trimer has three potential binding sites for xanthophyll cycle carotenoids (Liu et al., 2004). However, in principal, any of the light-harvesting antenna complexes could provide the NPQ site (Wentworth et al., 2004). Previous work with CP26-depleted plants showed little effect on NPQ (Andersson et al., 2001), whereas a small effect was found on NPQ in CP29-depleted plants. Here, we have shown in higher plants a dramatic reduction in NPQ upon removal of an antenna complex, CP24. This could suggest that CP24 provides the site of interaction with PsbS and zeaxanthin. The small reduction in NPQ in the absence of CP29 (Andersson et al., 2001) could be explained by the simultaneous partial reduction of CP24 in these plants. It is important to note that mRNA levels of genes coding for CP24 and CP29 during various conditions follow PsbS mRNA levels rather than *Lhcb1-3* and *Lhcb5* mRNA levels, suggesting that there is a regulatory module that coordinates the expression of PsbS, CP24, and CP29, somewhat different to the rest of the antenna polypeptides (Klimmek et al., 2006).

Substantial NPQ persists in the absence of CP24, and a saturating light intensity of 40% of the wild-type level of NPQ can be induced without CP24, so it seems unlikely that it provides a unique quenching site. Instead, the data point to a decrease in the efficiency of NPQ. Thus, the decrease in qE is due to the reduction in the amplitude of the more slowly forming component that is associated with the amplification of qE by violaxanthin deepoxidation (Crouchman et al., 2006). Two explanations can be offered: first, the decreased connectivity in the mutant plants may result in the decreased availability of subsaturating levels of the quencher; second, the generation of NPQ might be favored

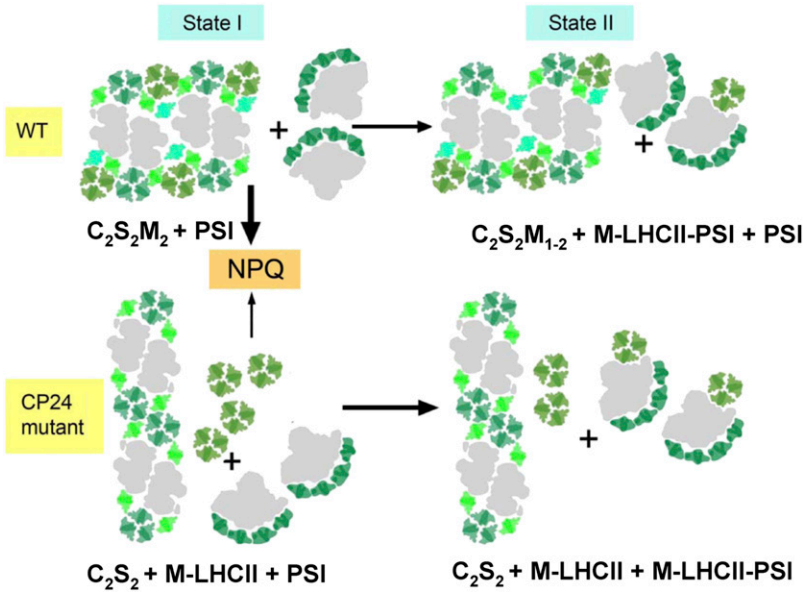

Figure 10. Model Showing How Lack of CP24 Affects the Macrostructure of the Antenna of PSII and the Regulation of Light Harvesting.

In State I, wild-type membranes contain the typical $C_2S_2M_2$ supercomplexes, which allow formation of large arrays of connected megacomplexes. In the grana of plants lacking CP24, head-to-tail megacomplexes of C_2S_2 supercomplexes are present, together with peripherally associated M-LHCII trimers. These two grana structures differ in their ability to form NPQ. In the transition to State II, there is detachment of M-trimers from PSII and their association with PSI. In the wild type, this results in appearance of some $C_2S_2M_1$ supercomplexes. In the plant lacking CP24, peripherally associated LHCII can more readily become associated with PSI, whereas in the wild type, the availability of M-trimers is restricted by their location within the supercomplexes. S-LHCII trimers are dark green, M-trimers are olive green, CP26 and CP29 are pale green, and CP24 is turquoise. Reaction center cores are in gray. Also shown are the subunits of LHCI, also in green.

by the optimal association of antenna complexes found in the $C_2S_2M_{1-2}$ macrostructure. It is unlikely that a change in connectivity could exert such a large change in NPQ– for the data shown in Table 2; the largest difference in fluorescence yield arising from the observed difference in connectivity was <10%. Since the quencher is not a stronger energy trap than the open reaction center (Li et al., 2004), change in connectivity from 1.5 to 0.9 could not produce a 60% difference in NPQ. Evidence in favor of the second explanation can be found in the observations that whenever the macrostructure is disturbed (by depletion of any antenna complex or by pigment deficiency), NPQ is reduced (Horton et al., 2005), albeit in some cases only slightly. Moreover, if quenching arises by conformational changes in an antenna complex, as proposed recently (Pascal et al., 2005), such events will be dependent on the local environment in the LHCII/PSII macrostructure.

It is interesting that the extent of NPQ and the amplitude of the psi-type CD band are strongly correlated when comparing wild-type, *koLhcb6*, and *asLhcb6* plants (Figure 5C), but neither is linearly related to the content of Lhcb6 protein. Indeed, the level of CP24 seems to be in excess of that required for normal structure and function of LHCII/PSII. Assuming that the CD signal is an indicator of the $C_2S_2M_2$-containing macrostructure, it is suggested that this organization can be maintained even if every complex does not bind CP24 (and an M-trimer). This is expected because $C_2S_2M_1$ complexes have been seen (Yakushevska et al., 2001) and models of the ordered arrays can accommodate less than stoichiometric M-trimers (Dekker and Boekema, 2005) and by inference CP24. Thus, both the long-range order, as indicated by CD, and NPQ are perhaps dependent not on CP24 per se but the C_2S_2M types of macrostructure.

Two Modes of the LHCII Structure and Function

We propose that there are two fundamental states of LHCII/PSII organization: the $C_2S_2M_2$ state and the C_2S_2 state (Figure 10). The former is essential for efficient light harvesting by PSII and for efficient NPQ, and it establishes the characteristics of the state transition. It requires CP24 and the M-LHCII trimer. In this mode, not only is LHCIIb fully coupled to PSII, but it is in the appropriate form to undergo transition to the quenched state. This may include proximity to the NPQ active factor PsbS and/or the provision of a membrane environment allowing flexibility in LHCII structure. The association of LHCIIb trimers from adjacent supercomplexes may be essential for NPQ, forming a CP24/PsbS/LHCII/zeaxanthin quenching locus. The second mode, C_2S_2, is characterized by less-efficient PSII light harvesting and in wild-type higher plants represents only a fraction of the PSII population (Yakushevska et al., 2001; Kouril et al., 2005). This mode is proposed to have a reduced efficiency of NPQ formation. In wild-type plants, the transition to State II involves the removal of M-trimers, resulting in mainly $C_2S_2M_1$ supercomplexes; in theory, some C_2S_2 supercomplexes could be formed, although significant numbers of these were not found in wild-type *Arabidopsis* (Kouril et al., 2005).

It is interesting to note the resemblance between the thylakoids of the CP24 mutants and those of *Chlamydomonas reinhardtii*. This alga lacks CP24 (Stauber et al., 2003) and contains only C_2S_2 complexes (Dekker and Boekema, 2005). Rapidly reversible NPQ is smaller and slower than that found in higher plants and less dependent on violaxanthin deepoxidation (Niyogi et al., 1997). NPQ in *Chlamydomonas* also appears to depend upon an LHCII trimer (Elrad et al., 2002), but it is controlled differently, possibly via phosphorylation of CP29 (Turkina et al., 2006). *Chlamydomonas* shows larger and more rapid state transitions compared with higher plants (Delosme et al., 1996), involving dissociation of LHCII and CP29 from PSII (Takahashi et al., 2006), probably involving the tightly bound S-trimer (Turkina et al., 2006). It has been concluded that the evolution of a light-harvesting antenna that fulfils the dual function of efficient light harvesting and effective photoprotection has been accompanied by the development of specific antenna complexes that confer characteristic structural arrangements in the grana membranes. In higher plants, the evolution of CP24 was a pivotal part of this process.

METHODS

Plant Materials

Arabidopsis thaliana cv Columbia expressing an antisense construct for the *Lhcb6* gene (*asLhcb6*) has been described previously (Ganeteg et al., 2004). The single antisense line presented a range of expression of the antisense phenotype in the plant population. A T-DNA knockout mutant (SALK_077953; N577953) with insertion into the *Lhcb6* gene (At1g15820) was obtained from the ABRC. To obtain plants homozygous for the insertion, plants were selfed and the progeny was screened with PCR and protein gel blotting using a monospecific Lhcb6 antibody. For amplification of the wild-type allele of *Lhcb6*, PCR primers with the sequences 5′-AGAAAAGCCGGGTCTTTCCCCAAAC-3′ and 5′-ACGCAATAAGCCACATAATGCAGCC-3′ were used, giving rise to a 900-bp fragment, and for identification of the knockout allele, the primers 5′-ACGCAATAAGCCACATAATGCAGCC-3′ and 5′-TGGTTCACGTAGTGGGCCATCG-3′ (LBa1) were used, yielding an 800-bp fragment. All plants were grown for 8 to 9 weeks in Conviron climate chambers with an 8-h photoperiod with a light intensity of 200 μmol photons m^{-2} s^{-1} and at day/night temperatures of 22/15°C. Thylakoids were prepared from fully expanded leaves as described by Ruban et al. (2006).

CD Spectroscopy

The CD spectra were recorded between 400 and 750 nm at room temperature in a J810 dichrograph (Jasco) using a band-pass of 3 nm and a resolution of 1 nm. The chlorophyll content of the thylakoid membrane was adjusted to 20 μg/mL and was measured in a glass cuvette with a 1-cm optical path length. Intact leaves were placed perpendicularly to the optical path. In the case of leaves, four to nine spectra were averaged to improve the signal-to-noise ratio.

Fluorescence Spectroscopy

Low-temperature spectroscopy was performed using an Optistat^{DN} LN-2 cooled bath cryostat (Oxford Instruments). Samples were diluted in a medium containing 70% glycerol (w/v), 20 mM HEPES buffer, pH 7.8, 5 mM $MgCl_2$, and 0.33 M sorbitol. The chlorophyll concentration was 1 μM. Fluorescence emission and excitation spectra were recorded using a SPEX FluoroLog FL3-22 spectrofluorimeter (SPEX Industries) as described previously (Ruban et al., 2006). The excitation light was provided from a Xenon light source. In fluorescence emission measurements, excitation was defined at 435 nm with a 5-nm spectral bandwidth. The

fluorescence spectral resolution was 1 nm. In fluorescence excitation measurements, fluorescence was detected at 695 nm with a 5-nm spectral bandwidth. The excitation spectral resolution was 1 nm. Spectra were automatically corrected for the spectral distribution of the exciting light during data acquisition.

Chlorophyll Fluorescence Induction

Fast fluorescence induction curves were recorded for detached, dark-adapted leaves vacuum infiltrated with 100 μM DCMU. A Dual PAM100 chlorophyll fluorescence photosynthesis analyzer (Heinz Walz) was used. Fluorescence was measured using the DUAL DB head with the instrument operated in the fast kinetics mode. Actinic illumination (1000 μmol photons m^{-2} s^{-1}) was provided by two arrays of 635-nm LEDs illuminating both the adaxial and abaxial surfaces of the leaf, applied 1 ms after turning on the 460-nm measuring beam. The measured fluorescence induction obtained in 20-ms induction curves (2000 points) was numerically fitted by the function $F(t,I,\sigma_{PSII},J)$ based on a sigmoidal fluorescence induction model (Koblizek et al., 2001), where J is the connectivity parameter that determines the shape of the curve, and σ_{PSII} is the functional cross section of PSII.

For analysis of NPQ, the fluorescence was measured with a pulse-modulated PAM-101 chlorophyll fluorometer (Heinz Walz). The plants were adapted in the dark for 30 min prior to measurement. Fluorescence quenching was induced by 10 min of actinic illumination with white light obtained from a KL1500 lamp (Heinz Walz) at various intensities. The maximal fluorescence in the dark-adapted state (Fm) and during the course of actinic illumination (Fm′) and the subsequent dark relaxation period were determined by a 0.8-s saturating (4000 μmol photons m^{-2} s^{-1}) light pulse applied at 1- to 2-min intervals. NPQ was defined as $Fm/Fm' - 1$. The reversible component (relaxing within 10 min) was assigned to energy-dependent NPQ (qE) and was calculated as $Fm/Fm' - Fm/Fm''$, where Fm′′ is the maximal yield of fluorescence after 10 min of dark relaxation following the actinic illumination.

State transition experiments were performed using leaf disks according to established protocols (Haldrup et al., 2001). Preferential PSII excitation was provided by illumination with red light at an intensity of 50 μmol photons m^{-2} s^{-1} provided by a KL1500 lamp equipped with a 650-nm interference filter, and excitation of PSI was achieved using far-red light from an LED light source (Heinz Walz; 102-FR) applied for 15 min simultaneously with red light. Periods of red + far-red and red light conditions were used alternately in several cycles, and the Fm level in State I (Fm^{I}) and State II (Fm^{II}) was determined at the end of each cycle by the application of a saturating light pulse as described above.

Polypeptide Analysis

Thylakoid proteins were analyzed using immunoblotting essentially as described by Ganeteg et al. (2001). For detailed measurements of CP24 content in the different plants, leaf disks with 8-mm diameters were homogenized in 250 μL 2× Laemmli buffer, and the homogenates were incubated at 90°C for 5 min followed by a 20-min incubation at 37°C and then proteins were separated by 15% denaturing SDS-PAGE (Laemmli, 1970). Two microliters of samples were loaded per lane. Chemiluminescence was detected on Hyperfilm ECL photographic film (Amersham Pharmacia). The developed film was digitalized and analyzed by the Image Master gel documentation system (Amersham Pharmacia) equipped with a Umax Powerlook III high-resolution scanner and 1D software package.

Pigment Analysis

The composition of carotenoids was determined by reverse phase HPLC (Farber et al., 1997). Leaf discs with equal areas were cut and frozen in liquid nitrogen and then homogenized in 100% acetone. Pigments were separated using a LiChrospher 100 RP-18 column with 5-μm particle size (Merck) and a Dionex HPLC. Twenty microliters of acetone extract was injected in the column, and the pigments were eluted by a gradient from solvent A (acetonitrile, methanol, and 0.1 M Tris/NaOH, pH 8.0, in a ratio of 87:10:3) to solvent B (4:I mixture of methanol and hexane). The gradient from solvent A to solvent B was run from 9 to 12.5 min at a flow rate of 2 mL/min. The amount of pigments was calculated from the integrated area of the corresponding peak using Chromeleon software (Dionex). The chlorophyll *a* and *b* contents on a leaf area basis were determined from leaf extracts according to the method described by Porra et al. (1989).

FPLC Analysis of Thylakoid Membranes

FPLC analysis was performed on detergent-solubilized, freshly prepared thylakoid membranes as described previously (Ruban et al., 2006). Thylakoids were suspended to a final chlorophyll concentration of 1.0 mg/mL and partially solubilized by the addition of *n*-dodecyl α-D-maltoside to a final concentration of 0.6 ot 0.8% (as specified in the text) and incubated for 1 min at room temperature. Unsolubilized material was removed by 1 min of centrifugation at 16,000 *g*. The supernatant was then filtered through a 0.45-μm filter and subjected to gel filtration chromatography using an Amersham-Pharmacia Äcta purifier system, including a Superdex 200 HR 10/30 column, following the protocol described by van Roon et al. (2000).

Electron Microscopy and Image Analysis

Samples were negatively stained with 2% uranyl acetate on glow discharged carbon-coated copper grids. Electron microscopy was performed on a Philips CM120FEG electron microscope equipped with a field emission gun operated at 120 kV. Images were recorded with a Gatan 4000 SP 4K slow-scan CCD camera at ×80,000 magnification at a pixel size (after binning the images) of 0.375 nm at the specimen level with GRACE software for semi-automated specimen selection and data acquisition (Oostergetel et al., 1998). Single particle analysis, including multi-reference and nonreference procedures, multivariate statistical analysis, and classification, was performed as previously (Boekema et al., 1999a).

ACKNOWLEDGMENTS

This work was supported by grants from the Biotechnology and Biological Sciences Research Council of the United Kingdom, the Swedish Research Council for Environment, Agricultural Sciences, and Spatial Planning, and the INTRO2 European Union FP6 Marie Curie Research Training Network. L.K. was a recipient of a Marie Curie Research Fellowship.

Received July 7, 2006; revised October 16, 2006; accepted October 31, 2006; published November 17, 2006.

REFERENCES

Allen, J.F. (1992). Protein-phosphorylation in regulation of photosynthesis. Biochim. Biophys. Acta **1098,** 275–335.

Allen, J.F., and Forsberg, J. (2001). Molecular recognition in thylakoid structure and function. Trends Plant Sci. **6,** 317–326.

Anderson, J.M., Chow, W.S., and Park, Y.I. (1995). The grand design of photosynthesis: Acclimation of the photosynthetic apparatus to environmental cues. Photosynth. Res. **46,** 129–139.

Andersson, J., Walters, R.G., Horton, P., and Jansson, S. (2001). Antisense inhibition of the photosynthetic antenna proteins CP29 and CP26: Implications for the mechanism of protective energy dissipation. Plant Cell **13,** 1193–1204.

Andersson, J., Wentworth, M., Walters, R.G., Howard, C.A., Ruban, A.V., Horton, P., and Jansson, S. (2003). Absence of the Lhcb1 and Lhcb2 proteins of the light-harvesting complex of photosystem II - Effects on photosynthesis, grana stacking and fitness. Plant J. **35,** 350–361.

Barzda, V., Mustardy, L., and Garab, G. (1994). Size dependency of circular dichroism in macroaggregates of photosynthetic pigment-protein complexes. Biochemistry **33,** 10837–10841.

Bassi, R., and Caffarri, S. (2000). Lhc proteins and the regulation of photosynthetic light harvesting function by xanthophylls. Photosynth. Res. **64,** 243–256.

Boekema, E.J., van Breemen, J.F.L., van Roon, H., and Dekker, J.P. (2000). Arrangement of photosystem II supercomplexes in crystalline macrodomains within the thylakoid membrane of green plant chloroplasts. J. Mol. Biol. **301,** 1123–1133.

Boekema, E.J., van Roon, H., Calkoen, F., Bassi, R., and Dekker, J.P. (1999a). Multiple types of association of photosystem II and its light-harvesting antenna in partially solubilized photosystem II membranes. Biochemistry **38,** 2233–2239.

Boekema, E.J., van Roon, H., van Breemen, J.F.L., and Dekker, J.P. (1999b). Supramolecular organization of photosystem II and its light-harvesting antenna in partially solubilized photosystem II membranes. Eur. J. Biochem. **266,** 444–452.

Briantais, J.M., Vernotte, C., Picaud, M., and Krause, G.H. (1979). A quantitative study of the slow decline of chlorophyll a fluorescence in isolated chloroplasts. Biochim. Biophys. Acta **548,** 128–138.

Camm, E.L., and Green, B.R. (1989). The chlorophyll a/b complex, Cp29, is associated with the photosystem II reaction center core. Biochim. Biophys. Acta **974,** 180–184.

Crouchman, S., Ruban, A., and Horton, P. (2006). PsbS enhances nonphotochemical fluorescence quenching in the absence of zeaxanthin. FEBS Lett. **580,** 2053–2058.

Dekker, J.P., and Boekema, E.J. (2005). Supramolecular organization of thylakoid membrane proteins in green plants. Biochim. Biophys. Acta **1706,** 12–39.

Delosme, R., Olive, J., and Wollman, F.A. (1996). Changes in light energy distribution upon state transitions: An in vivo photoacoustic study of the wild type and photosynthesis mutants from *Chlamydomonas reinhardtii.* Biochim. Biophys. Acta **1273,** 150–158.

Demmig-Adams, B. (1990). Carotenoids and photoprotection: A role for the xanthophyll zeaxanthin. Biochim. Biophys. Acta **1020,** 1–24.

Dobrikova, A.G., Varkonyi, Z., Krumova, S.B., Kovacs, L., Kostov, G.K., Todinova, S.J., Busheva, M.C., Taneva, S.G., and Garab, G. (2003). Structural rearrangements in chloroplast thylakoid membranes revealed by differential scanning calorimetry and circular dichroism spectroscopy. Thermo-optic effect. Biochemistry **42,** 11272–11280.

Elrad, D., Niyogi, K.K., and Grossman, A.R. (2002). A major light-harvesting polypeptide of photosystem II functions in thermal dissipation. Plant Cell **14,** 1801–1816.

Farber, A., Young, A.J., Ruban, A.V., Horton, P., and Jahns, P. (1997). Dynamics of xanthophyll-cycle activity in different antenna subcomplexes in the photosynthetic membranes of higher plants - The relationship between zeaxanthin conversion and nonphotochemical fluorescence quenching. Plant Physiol. **115,** 1609–1618.

Finzi, L., Bustamante, C., Garab, G., and Juang, C.B. (1989). Direct observation of large chiral domains in chloroplast thylakoid membranes by differential polarization microscopy. Proc. Natl. Acad. Sci. USA **86,** 8748–8752.

Ganeteg, U., Kulheim, C., Andersson, J., and Jansson, S. (2004). Is each light-harvesting complex protein important for plant fitness? Plant Physiol. **134,** 502–509.

Ganetag, U., Strand, Å., Gustafsson, P., and Jansson, S. (2001). The properties of the chlorophyll a/b-binding proteins Lhca2 and Lhca3 studied in vivo using antisense inhibition. Plant Physiol. **127,** 150–158.

Garab, G., Cseh, Z., Kovacs, L., Rajagopal, S., Varkonyi, Z., Wentworth, M., Mustardy, L., Der, A., Ruban, A.V., Papp, E., Holzenburg, A., and Horton, P. (2002). Light-induced trimer to monomer transition in the main light-harvesting antenna complex of plants: Thermo-optic mechanism. Biochemistry **41,** 15121–15129.

Garab, G., Wells, S., Finzi, L., and Bustamante, C. (1988). Helically organized macroaggregates of pigment-protein complexes in chloroplasts: Evidence from circular intensity differential scattering. Biochemistry **27,** 5839–5843.

Green, B.R., and Durnford, D.G. (1996). The chlorophyll-carotenoid proteins of oxygenic photosynthesis. Annu. Rev. Plant Physiol. Plant Mol. Biol. **47,** 685–714.

Haldrup, A., Jensen, P.E., Lunde, C., and Scheller, H.V. (2001). Balance of power: A view of the mechanism of photosynthetic state transitions. Trends Plant Sci. **6,** 301–305.

Holt, N.E., Fleming, G.R., and Niyogi, K.K. (2004). Toward an understanding of the mechanism of nonphotochemical quenching in green plants. Biochemistry **43,** 8281–8289.

Horton, P., and Ruban, A. (2005). Molecular design of the photosystem II light-harvesting antenna: Photosynthesis and photoprotection. J. Exp. Bot. **56,** 365–373.

Horton, P., Ruban, A.V., and Walters, R.G. (1996). Regulation of light harvesting in green plants. Annu. Rev. Plant Physiol. Plant Mol. Biol. **47,** 655–684.

Horton, P., Wentworth, M., and Ruban, A. (2005). Control of the light harvesting function of chloroplast membranes: The LHCII-aggregation model for non-photochemical quenching. FEBS Lett. **579,** 4201–4206.

Jansson, S. (1994). The light-harvesting chlorophyll a/b binding proteins. Biochim. Biophys. Acta **1184,** 1–19.

Keller, D., and Bustamante, C. (1986). Theory of the interaction of light with large inhomogeneous molecular aggregates. 2. Psi-type circular dichroism. J. Chem. Phys. **84,** 2972–2980.

Klimmek, F., Sjodin, A., Noutsos, C., Leister, D., and Jansson, S. (2006). Abundantly and rarely expressed Lhc protein genes exhibit distinct regulation patterns in plants. Plant Physiol. **140,** 793–804.

Koblizek, M., Kaftan, D., and Nedbal, L. (2001). On the relationship between the non-photochemical quenching of the chlorophyll fluorescence and the photosystem II light harvesting efficiency. A repetitive flash fluorescence induction study. Photosynth. Res. **68,** 141–152.

Kouril, R., Zygadlo, A., Arteni, A.A., de Wit, C.D., Dekker, J.P., Jensen, P.E., Scheller, H.V., and Boekema, E.J. (2005). Structural characterization of a complex of photosystem I and light-harvesting complex II of *Arabidopsis thaliana.* Biochemistry **44,** 10935–10940.

Laemmli, U.K. (1970). Cleavage of structural proteins during the assembly of the head of bacteriophage T4. Nature **227,** 680–685.

Lavergne, J., and Trissl, H.W. (1995). Theory of fluorescence induction in photosystem II: Derivation of analytical rxpressions in a model including exciton-radical-pair equilibrium and restricted energy transfer between photosynthetic units. Biophys. J. **68,** 2474–2492.

Lazar, D. (1999). Chlorophyll a fluorescence induction. Biochim. Biophys. Acta **1412,** 1–28.

Li, X.P., Bjorkman, O., Shih, C., Grossman, A.R., Rosenquist, M., Jansson, S., and Niyogi, K.K. (2000). A pigment-binding protein essential for regulation of photosynthetic light harvesting. Nature **403,** 391–395.

Li, X.P., Gilmore, A.M., Caffarri, S., Bassi, R., Golan, T., Kramer, D., and Niyogi, K.K. (2004). Regulation of photosynthetic light harvesting

involves intrathylakoid lumen pH sensing by the PsbS protein. J. Biol. Chem. **279,** 22866–22874.

Liu, Z., Yan, H., Wang, K., Kuang, T., Zhang, J., Gui, L., An, X., and Chang, W. (2004). Crystal structure of spinach major light-harvesting complex at 2.72 A resolution. Nature **428,** 287–292.

Montane, M.H., Tardy, F., Kloppstech, K., and Havaux, M. (1998). Differential control of xanthophylls and light-induced stress proteins, as opposed to light-harvesting chlorophyll a/b proteins, during photosynthetic acclimation of barley leaves to light irradiance. Plant Physiol. **118,** 227–235.

Nedbal, L., Trtilek, M., and Kaftan, D. (1999). Flash fluorescence induction: A novel method to study regulation of photosystem II. J. Photochem. Photobiol. B **48,** 154–157.

Niyogi, K.K., Bjorkman, O., and Grossman, A.R. (1997). Chlamydomonas xanthophyll cycle mutants identified by video imaging of chlorophyll fluorescence quenching. Plant Cell **9,** 1369–1380.

Oostergetel, G.T., Keegstra, W., and Brisson, A. (1998). Automation of specimen selection and data acquisition for protein electron crystallography. Ultramicroscopy **74,** 47–59.

Pascal, A.A., Liu, Z., Broess, K., van Oort, B., van Amerongen, H., Wang, C., Horton, P., Robert, B., Chang, W., and Ruban, A. (2005). Molecular basis of photoprotection and control of photosynthetic light-harvesting. Nature **436,** 134–137.

Peter, G.F., and Thornber, J.P. (1991). Biochemical composition and organization of higher-plant photosystem II light-harvesting pigment proteins. J. Biol. Chem. **266,** 16745–16754.

Porra, R.J., Thompson, W.A., and Kriedemann, P.E. (1989). Determination of accurate extinction coefficients and simultaneous equations for assaying chlorophyll a and chlorophyll b extracted with 4 different solvents - Verification of the concentration of chlorophyll standards by atomic absorption spectroscopy. Biochim. Biophys. Acta **975,** 384–394.

Ruban, A.V., Pascal, A., and Robert, B. (2000). Xanthophylls of the major photosynthetic light-harvesting complex of plants: Identification, conformation and dynamics. FEBS Lett. **477,** 181–185.

Ruban, A.V., Solovieva, S., Lee, P.J., Ilioaia, C., Wentworth, M., Ganeteg, U., Klimmek, F., Chow, W.S., Anderson, J.M., Jansson, S., and Horton, P. (2006). Plasticity in the composition of the light harvesting antenna of higher plants preserves structural integrity and biological function. J. Biol. Chem. **281,** 14981–14990.

Ruban, A.V., Wentworth, M., Yakushevska, A.E., Andersson, J., Lee, P.J., Keegstra, W., Dekker, J.P., Boekema, E.J., Jansson, S., and Horton, P. (2003). Plants lacking the main light-harvesting complex retain photosystem II macro-organization. Nature **421,** 648–652.

Simidjiev, I., Barzda, V., Mustardy, L., and Garab, G. (1997). Isolation of lamellar aggregates of the light-harvesting chlorophyll a/b protein complex of photosystem II with long-range chiral order and structural flexibility. Anal. Biochem. **250,** 169–175.

Stauber, E.J., Fink, A., Markert, C., Kruse, O., Johanningmeier, U., and Hippler, M. (2003). Proteomics of *Chlamydomonas reinhardtii* light-harvesting proteins. Eukaryot. Cell **2,** 978–994.

Takahashi, H., Iwai, M., Takahashi, Y., and Minagawa, J. (2006). Identification of the mobile light-harvesting complex II polypeptides for state transitions in *Chlamydomonas reinhardtii.* Proc. Natl. Acad. Sci. USA **103,** 477–482.

Turkina, M.V., Kargul, J., Blanco-Rivero, A., Vilrejo, A., Barber, J., and Vener, A.V. (2006). Environmentally modulated phosphoproteome of photosynthetic membranes in the green alga *Chlamydomonas reinhardtii.* Mol. Cell. Proteomics **5,** 1412–1425.

van Roon, H., van Breemen, J.F.L., de Weerd, F.L., Dekker, J.P., and Boekema, E.J. (2000). Solubilization of green plant thylakoid membranes with n-dodecyl-alpha,D-maltoside. Implications for the structural organization of the Photosystem II, Photosystem I, ATP synthase and cytochrome b(6)f complexes. Photosynth. Res. **64,** 155–166.

Walters, R.G., Ruban, A.V., and Horton, P. (1996). Identification of proton-active residues in a higher plant light-harvesting complex. Proc. Natl. Acad. Sci. USA **93,** 14204–14209.

Wentworth, M., Ruban, A.V., and Horton, P. (2004). The functional significance of the monomeric and trimeric states of the photosystem II light harvesting complexes. Biochemistry **43,** 501–509.

Yakushevska, A.E., Jensen, P.E., Keegstra, W., van Roon, H., Scheller, H.V., Boekema, E.J., and Dekker, J.P. (2001). Supermolecular organization of photosystem II and its associated light-harvesting antenna in *Arabidopsis thaliana.* Eur. J. Biochem. **268,** 6020–6028.

Yakushevska, A.E., Keegstra, W., Boekema, E.J., Dekker, J.P., Andersson, J., Jansson, S., Ruban, A.V., and Horton, P. (2003). The structure of photosystem II in Arabidopsis: Localization of the CP26 and CP29 antenna complexes. Biochemistry **42,** 608–613.